UCRL-16955

University of California

Ernest O. Lawrence Radiation Laboratory

STRAIN CONTRAST IMAGES FROM SMALL DEFECTS

TWO-WEEK LOAN COPY

This is a Library Circulating Copy
which may be borrowed for two weeks.
For a personal retention copy, call
Tech. Info. Division, Ext. 5545

Berkeley, California

DISCLAIMER

This document was prepared as an account of work sponsored by the United States Government. While this document is believed to contain correct information, neither the United States Government nor any agency thereof, nor the Regents of the University of California, nor any of their employees, makes any warranty, express or implied, or assumes any legal responsibility for the accuracy, completeness, or usefulness of any information, apparatus, product, or process disclosed, or represents that its use would not infringe privately owned rights. Reference herein to any specific commercial product, process, or service by its trade name, trademark, manufacturer, or otherwise, does not necessarily constitute or imply its endorsement, recommendation, or favoring by the United States Government or any agency thereof, or the Regents of the University of California. The views and opinions of authors expressed herein do not necessarily state or reflect those of the United States Government or any agency thereof or the Regents of the University of California.

Harwell Conf.
July 1966

UCRL-16955

UNIVERSITY OF CALIFORNIA
Lawrence Radiation Laboratory
Berkeley, California

AEC Contract W-7405-eng-48

STRAIN CONTRAST IMAGES FROM SMALL DEFECTS

W. L. Bell, D. M. Maher, and G. Thomas

July 1966

STRAIN CONTRAST IMAGES FROM SMALL DEFECTS+

W. L. Bell, D. M. Maher, and G. Thomas

Inorganic Materials Research Division, Lawrence Radiation Laboratory
and Department of Mineral Technology, College of Engineering
University of California, Berkeley, California

Abstract

The purpose of this paper is to illustrate the optimum experimental conditions necessary for obtaining strain contrast images from various types of defects. The results are discussed in terms of existing theory. Defects of known character in a number of systems have been employed. The parameters which have been considered for both the bright and dark field case are: the foil thickness, the extinction distance, the deviation parameter, the anomalous absorption parameter, defect size, defect shape, defect position in the foil, inclination of the defect with respect to the incident beam, defect density and the operating reflection.

Whilst the shape and displacement vector associated with a defect can be obtained uniquely under the appropriate orientations and diffracting conditions, it is rarely that the sense of the displacements of small defects can be found uniquely from the image and its relation to the direction of $\bar{g}$, even though defects of known character, e.g., precipitates and dislocation loops, have been examined in detail. Thus at this time it does not seem possible to unambiguously determine vacancy and interstitial type strain fields using strain contrast imaging except for the special case of defects lying at, or intersecting, the surface.

+ Paper presented at the Harwell Conference July 1966.

Extension of the existing theory is needed in order to permit a reliable interpretation of the defect character. It is suggested that more detailed consideration be given to the defect model and the various parameters which affect the image characteristics in a particular crystal, and that measured parameters characteristic of the crystal be employed whenever possible, so that a closer correspondence can be established between theory and particular experimental situations.

I. INTRODUCTION

There are several problems associated with the detection and identification of small defects by electron microscopy and diffraction. The question of resolution depends on whether or not a defect produces lattice strains.[1,2] In the absence of strain fields, incoherent scattering largely determines the resolution limit and, in such cases, with current instruments and techniques, defects smaller that 10-20Å in size are difficult to resolve. Non strain producing defects are of relatively minor occurrence, they are usually found in alloys containing component atoms of similar size, e.g. GP zones in Al-Ag.[3] The contrast mechanism in these cases is that of "mass thickness scattering", i.e., the defect produces an effective thickness change Δt in a foil of thickness t. This effective thickness change is due to the differences in extinction distances and absorbing power between the defect and the matrix.

The majority of defects in crystals produce strain fields, for example, prismatic dislocation loops or point defect aggregates introduced by quenching (and aging), irradiation, plastic deformation, and precipitates in alloys. In these cases, defects can often be detected by diffraction contrast,[4-7] and information regarding the size and displacement vector of the defect can be found by bright-field imaging using $\bar{g}.\bar{R}$. contrast experiments. However, when the defects are small (less than 100-200Å dia.) strain contrast imaging must be done under critical conditions,[1,2] and usually in high resolution dark-field.

Images of defects near the foil surface, obtained when a set of

diffracting planes are at or very close to the Bragg reflecting condition, will be "anomalously wide" with respect to the actual size of the defect.[1] The images generally exhibit intensity fluctuations above and below background intensity which are characteristic of the nature of the defect, and appear as dark and light lobes. These images are referred to as strain contrast images because under the conditions specified[1,2] the phases of electrons travelling through the crystal and the distribution of electrons on the upper and lower dispersion surfaces[4-6] are markedly affected by very small strains in the lattice, either from short range, small strains at or near the defect, or due to large, long-range strain fields from a distant defect.

Theoretically it is possible to use a strain contrast image to characterize the magnitude and direction of the displacement vector $\bar{R}$ and also the shape, size and character of a defect (i.e. whether it has a vacancy or interstitial type strain field). In practice it has been found that whilst information regarding $\bar{R}$, size, and shape of the defect is relatively easily found,[1,2,8-11, for review see Ref. 8] the character of the defect may not easily be determined uniquely. In fact, complicated and conflicting results are often obtained. This is unfortunate because, for example, in irradiated or deformed crystals where both small vacancy and interstitial defects are produced, unique identification by strain contrast imaging will, in general, not be possible.

In the case of small precipitates, detection is often facilitated by observation of the diffraction pattern if one utilizes the effect

of the shape factor on the scattered intensities, e.g. thin plates produce streaked patterns,[3] small needles produce intensity discs which appear as curved streaks on the pattern.[13] However, in this paper we shall primarily be concerned with the experimental conditions governing strain contrast images, and in particular visibility and character of defects.

Theoretical bases have been established for explaining contrast from spherical and planar defects when observed under conditions where anomalous absorption plays an important role in determining the image properties.[1,2] In order to facilitate detection, (in general) high resolution (gun tilted) dark field images[10] should be used to minimize spherical and chromatic aberration. However, it will be demonstrated that many photographs of the same area obtained for several different imaging conditions must be obtained in order to evaluate the possible interpretations. The usual geometrical factors must be accounted for in comparing bright field and dark field images with their diffraction patterns.[7,10]

We should also draw attention to the fact that small defects can be produced as a result of ion damage inside the microscope[14,15] or from electropolishing the foils,[16] unless care is exercised in the experimental technique.

The purpose of this paper is to illustrate, using defects of known character in a number of systems, the experimental conditions which affect the observation of strain contrast images and the relationship of these observations to existing theory. Some of the more important parameters to be considered are: the foil thickness,

the extinction distance, the anomalous absorption parameter, the macroscopic deviation from the exact Bragg condition, defect characteristics such as size, shape, position in the foil, and its inclination with respect to the incident beam, and the density of defects in a material being studied. Some consideration will also be given to the bright and dark field imaging relations.

The defects and systems to be considered are: polishing pits in an Ag_2Al alloy, Frank loops and perfect prismatic loops in quenched aluminum foils, vacancy type platelike zones in Al-4%Cu alloy,[3] interstitial type rodlike defects in an Al-Mg_2Si alloy[12] and also doped silicon wafers.

II. FOIL THICKNESS

Most theoretical predictions deal with strain contrast images at the Bragg position and intensity profiles have been calculated to show these images at this condition.[1,2] These profiles are usually obtained for defects in a foil an integral number of extinction distances thick. Under this assumption the bright-field background intensity is a maximum and the dark-field background intensity is a minimum. The absorption parameters of the crystal are what determine, in a perfect foil, the maximum and minimum intensity levels obtainable in a foil of given thickness.[17,18] If a change of phase of the electron wave in the vicinity of a defect were all that occurred, only black images on a white background in bright-field and what images on a black back-

ground in dark-field would be observed. However, a simple phase change is not all that the electron wave experiences in passing the neighborhood of a defect. Along with the change of phase, there generally occurs a redistribution of the dispersed wave components which, theoretically at least, entails the possibility of either more or less absorption occuring in a given thickness of foil. Furthermore, local rotations of the lattice occur in the vicinity of a defect which are accounted for in the dynamical equations[5,6] as the rate of change of the displacement function. That is, there are in effect local deviations from the Bragg conditions which are satisfied by the surrounding foil, i.e. s varies in this region.* Also, no consideration has been given to the effects of local changes in interplanar spacing around the defect. Such changes must change the scattering factor.

Since the amplitude coefficients of the dispersed waves in both the transmitted and diffracted directions are functions of a geometrical deviation parameter, as are the phase factors and the anomalous absorption factors, the intensity in a given thickness of foil can be caused to vary from background by this second mechanism, due to the presence of a defect. In the case of defects which are small compared to the thickness of the foil and whose strain fields are well localized, it would be reasonable to expect that no great intensity fluctuations would occur above or below background when this background intensity is a maximum or minimum, respectively, for a

---

*s is the deviation of the reciprocal lattice point from the reflecting sphere. $s < 0$ represents the reciprocal lattice point to be outside the sphere.

perfect foil an integral number of extinction distances thick at the Bragg condition. The theoretical profiles presented[17,18] are, therefore, not determined for the best experimental conditions, nor would be curves calculated for foil thicknesses of an odd number of half extinction distances, for the same reasons. The best image contrast is found to be in regions between extreme background intensity extrema, i.e., in foils for which the thickness is an odd number of quarter extinction distances.[10] One qualification is that in thick foils, due to anomalous absorption,[17] the minimum background intensity is not much lower than the maximum background intensity and is considerably above that level that would be present if there were only mean linear absorption occurring in the crystal. Thus, intensity fluctuations below background of the same order of magnitude as that above background can occur.[19] An example of this is shown in Fig. 1; the material is quenched aluminum and bright-field and dark-field images are shown from a wedge shaped region. Notice that in almost every instance where a defect is located in a region of the foil where the background intensity is a maximum, the strain contrast images are of poor quality and generally only a black image is observable. In the thinner region of the foil where the intensity minima provide the darkest background, the defect images are primarily white. The background intensity minima are, of course, not nearly as low in the thicker region of the foil and therefore, defect images can be obtained which have better contrast. The defect images at foil thicknesses of an odd number of quarter extinction distances are most always of good contrast.

III. EXTINCTION DISTANCE

The thickness of a foil in a given region can effectively be changed by changing the extinction distance of the operating reflection responsible for contrast. This can be accomplished in two ways: firstly, for a given reflection at $s = 0$, the extinction distance can only be decreased by changing s, and secondly, the extinction distance can either be lengthened or shortened by changing the operating reflection to one of higher order or lower order, respectively.

The extinction distance for a set of reflecting planes varies according to the following relation:[4,5]

$$t_o' = \frac{t_o}{\sqrt{1 + s^2 t_o^2}}$$

where t_o = extinction distance at the Bragg angle and s = deviation parameter

Making the extinction distance shorter by varying the parameter s gives rise to certain advantages and disadvantages. Some of the advantages are: (1) defects which are located in a foil of such a thickness that the strain contrast images are of poor contrast can be made to exhibit good strain contrast by varying s by only a small amount, thereby, changing the local background intensity so that it is favorable, (2) defects which are so located in the crystal that, although near one surface of the foil they do not give rise to significant strain contrast at $s = 0$, they can be made to exhibit strong strain contrast images by a small change in s, (3) defects which lie near a particular surface can be selected using an appropriate sign of s for dark-field imaging techniques,[20] (4) the background intensity in dark-field images can be

sufficiently lowered that the phase contrast mechanism, combined with redistribution of the dispersed wave components and local lattice rotations, can be very effective in producing good strain contrast images even when the foil thickness is such as to give a maximum in background intensity for the operating value of s. Some of the disadvantages which occur are: (1) due to a decrease in anomalous transmission when $s \neq 0$, the level of diffuse scattered radiation contributing to the background is increased and both image contrast and image detail will be affected adversely, (2) since the bright-field intensity distribution is asymmetrical about $s = 0$, using non-zero values of s will cause the background to vary markedly from that obtained at the exact Bragg angle ($s = 0$), with the result that for $s > 0$ images will tend to be black on a white background and for $s < 0$ images will tend to be white on a dark background, (3) defects near the center of the foil will be less liable to detection by strain contrast imaging techniques, (4) in dark-field, defect images will not usually be representative of all defects throughout the thickness of the foil but will be restricted to defects only at or near one of the surfaces, (5) sufficiently large deviations from the Bragg angle will either bring about images which are nearly kinematical, since anomalous absorption no longer plays an important role in imaging formation, or it may bring about a situation which must be considered for the multi-beam case of diffraction (e.g. the symmetrical orientation at maximum value of s negative); (6) contrast reversals can occur.

There are also certain advantages or disadvantages in using different order reflections for obtaining different extinction distances. The lower order beams, although having shortest extinction distances, are normally used since they are the most easily obtainable and provide better images. High order reflections, having long extinction distances are preferable for most strain contrast work, (see Section VII) but generally yield images of poor quality. It is, of course, necessary to use whatever reflections are available or are necessary to obtain contrast.

IV. ANOMALOUS ABSORPTION PARAMETER

The absorption distance is given by the relation:[17]

$$\xi_g' = \xi_g \sqrt{1 + t_o^2 s^2} \qquad \text{where } \xi_g = \text{minimum absorption distance}$$

and is a function of both the deviation parameter, s, and the extinction distance, and at $s = 0$ the absorption length should be independent of the operating reflection, i.e., a property of the crystal itself. We have found, in aluminum and in silicon, using the wedge fringe method for determining absorption constants for electrons, that the anomalous absorption parameter decreases only slightly for a given thickness of foil with increase in the order of reflection.[20] This follows from a consideration of the diffuse contribution to the background intensity which decreases with increasing angle of diffraction. Thus, we have the two parameters t_o and ξ_g both independent crystal parameters. One of the primary assumptions in the solution of the absorbing theory was that the quantity t_o/ξ_g be quite small, that is, that the absorption

distance be much larger than the extinction distance.[17] In the theoretical image profiles $t_o/\xi_g = 0.10$ is generally assumed, which appears to be a reasonable average value. However, it is clear that this is a hypothetical case and the parameter t_o/ξ_g increases linearly with the extinction distance and thus the two beam theory becomes slightly less accurate for higher order beams and more nearly accurate for low order beams. In the case of aluminum it is possible to consider a foil of a given thickness as a thick foil with weak anomalous absorption when a low order beam is used or as a thin foil with strong anomalous absorption when a high order beam is used for imaging. Figure 2 shows theoretical intensity profiles for wedge-shape foils using absorption parameters measured for different reflections in aluminum,[19] and illustrates, for the first four reflections, the comparable intensity fluctuations for distances up to ten (111) extinction distances. Defect images calculated for five extinction distances thick foils with $t_o/\xi_g = 0.10$ may more nearly correspond to thicker foils for low order beams and thinner foils for high order beams. In aluminum the theoretical intensity vs depth curves would correspond to about $9.8t_o$ for {111}, $7.7t_o$ for {200}, $3.9t_o$ for {220}, and $3.1t_o$ for {311} reflecting planes, respectively. Figure 2 shows that at these positions contrast would be poor indeed.

The point to be made here is that, theoretically, images will be obtained in foils sufficiently thick that defects near the center of the foil will not be visible and strong contrast will be obtained only from defects near the surfaces, whereas in reality defect images must be obtained when and where they can be found and the foil thickness is

generally an unknown parameter, but usually small and the operating reflections are usually of low order, and thus defects near the center of the foil should, usually, be readily visible. Ideally, one should have available theoretical curves compiled both for varying foil thicknesses with a given value of t_o/ξ_g and for varying values of t_o/ξ_g for given values of foil thicknesses.

V. DEVIATION PARAMETER

As far as the background is concerned, the s dependence of the intensity distribution is included in the parameter $w = st_o$. The amplitude coefficients of the dispersed waves in both the transmitted and diffracted directions are functions of this parameter. Figures 3a, b, and c illustrate how the theoretical wedge intensity profiles for the (111) beam in aluminum varies with s in bright-field; the minimum background decreases markedly for $s < 0$ and increases markedly for $s > 0$. Contrast in bright-field images will, therefore, tend to be white on black for $s < 0$ and black on white for $s > 0$. The Bragg position represents the position that should be near optimum for obtaining strain contrast images, since tilting or rotation of the lattice near a defect can cause either a local decrease or increase in the transmitted intensity from the background of the perfect crystal. Figures 3e, f illustrate a similar concept for the scattered intensity, but the minimum and maximum background levels decrease with increasing s, regardless of sign. Therefore, strain contrast images in regions where the background is a maximum should actually be of better quality for non-zero values of s, because, by redispersion of the wave components and rotation of

the lattice, the intensity near a defect can vary either up or down in these regions, whereas, it could not increase significantly at the Bragg angle.

The diffracted amplitudes are proportional to $1/\sqrt{1+w^2}$, thus, decreasing rapidly with w. The important point here is that, of two operating reflections, the one with the larger extinction distance will be more sensitive to changes in s, in the amplitude coefficients, the phase relationships, and the anomalous absorption parameter. This is illustrated for aluminum using the same region of a bent, wedge-shaped foil for the {111} reflection and for the {220} reflection in Fig. 4. The bright fringes in each case represent regions where $t\sqrt{\frac{1}{t_o^2} + s^2} - n$ an interger. For t_o small, the fringes are widely separated and contrast conditions vary slowly with changing s and t. For t_o large, the fringes are close together and contrast conditions vary rapidly. The regions in which contrast conditions can be considered kinematical are those for which $s^2 \gg 1/t^2$, and it is obvious that this occurs for smaller values of s for high order beams than for low order beams. This means that data obtained using high order reflections must be limited to angles very close to the exact Bragg angle to be useful as far as strain contrast theory goes. For example, the extinction distance varies roughly inversely with the square of the interplanar spacing, hence the kinematical region would be reached for a {222} reflection with a value of s about four times smaller than that necessary to make the {111} reflection kinematical.

In addition to obtaining the kinematical extinction distance $t_o' = 1/s$, more rapidly with beams having a large t_o, the non-anomalous absorption

length, $\xi'_g = \xi_g t_o s \rightarrow \infty$, is also obtained for much smaller values of s for such reflections than would be the case for reflections where t_o is small. In this respect, too, more care must be exercised when dealing with strain contrast images using high order beams.

The deviation parameter also plays an important role in determining, for defects distributing throughout the thickness of a foil, which defects will display the better image contrast. Defects near the center of the foil can usually be observed only when the foil is sufficiently thin and the macroscopic value of s is sufficiently close to zero. Defects near the surfaces will still be in good contrast for non-zero values of s, but there is an asymmetrical relationship between the sign of the parameter s and the surface near which defects will exhibit images which are in good contrast with respect to the background intensity.[20] Briefly stated, the dark-field asymmetrical imaging properties with s are as follows: based upon the theoretical image profiles for stacking faults, dislocations and dipoles, dark-field micrographs for $s > 0$ will exhibit their best contrast around defects near the lower surface of the foil; dark-field micrographs for $s < 0$ will exhibit their best contrast around defects near the upper surface of the foil. For the cases of stacking faults and dislocation lines inclined to and intersecting the surfaces of the foil, and also the case of large faulted loops these relationships have been shown to be valid.[20] The contrast decreases with increasing distance from the foil surface which is favored by the particular sign of the parameter s. Slip trace images and surface defects also faithfully obey these imaging rules.[21]

Application of these considerations have allowed the authors to

conclude that the defects obtained in quenched copper foils, reported elsewhere,[10] were, in most cases, distributed throughout the entire thickness of the foil since strain contrast images were obtained on both sides of bend contours. Thus, dark-field images obtained on both sides of a contour indicate immediately that defects exist throughout the foil thickness.

When these rules are extended to small defects, notice must be paid to the fact that if the size of the defect is small in comparison with the extinction distance of the operating reflection, there will be positions in the foil, even though they be near the surface preferred for contrast, where the defect images may exhibit poor contrast, (e.g. Fig. 1) perhaps weaker than that obtained from a defect near the other surface which is ideally located to exhibit weak strain contrast, or perhaps the defect may be completely undetectable because it is disadvantageously located in the foil. If the latter is the case, then s must be suitably increased or decreased so as to effect a change in extinction distance such that the defect is at a depth suitable for exhibiting a good strain contrast image or, alternatively, the operating reflection must be changed. Figure 5 shows a number of defects in quenched aluminum. Defect A must lie near the center of the foil since it is weakly visible only at $s = 0$ for the (200) reflection. Defects B and C are only very weakly visible at $s = 0$ in dark-field whereas they exhibit excellent strain contrast images for $s < 0$. Defect D is completely invisible at $s = 0$ in dark-field and then exhibits strong strain contrast at $s < 0$. Changing to a (220) reflection causes defect B to appear in good strain contrast and defect D to appear

only in weak dark contrast. Notice that the defects marked E reverse the direction of their black-white images upon changing from $s = 0$ to $s \neq 0$ in dark-field. The two defects at the centers of the circles in Fig. 6 can be used to illustrate image qualities of small defects for a wide range of the parameter s for both the (111) reflection and the (220) reflection. In (a) advantage is taken of the small extinction distance for (111) to vary s widely and still obtain good contrast. One of the defects is invisible at $s = 0$ and the other nearly so. The defect on the right exhibits strong strain contrast at some positive value of s and reverses its character upon increasing s still further, at which time the defect on the left becomes visible. When use is made of the (220) reflection in (b), it can be seen that it is extremely difficult to obtain strain contrast images except very near the exact Bragg condition and then the defect images reverse themselves on either side of the central maximum.

Because the absorption parameters are relatively independant of the operating reflection, these dark-field rules should be valid for all orders of reflection and indeed appear to be so for stacking faults and rodlike defects in silicon, observed using both a {111} and a {400} operating reflection for contrast.[20] However, there appears to be a dichotomy in aluminum containing loops after quenching. For the {200} reflection those defects appearing in good contrast for $s < 0$ are the exact opposite of those appearing for the {311} reflection for the same sign of s, and vice versa for $s > 0$ as shown in Fig. 7. The letters T and B indicate defects which are near the top or bottom surface, respectively,

as determined from the appropriate bright-field and dark-field micrographs taken at $s = 0$. Not all defects could be so characterized because the unfavorable background conditions would not allow a black-white image to be resolved except at foil thicknesses of odd-quarter numbers of extinction distances. However, it is clear from the defects marked, that they obey the dark-field asymmetry rule much more faithfully for the (200) reflection (Figs. 7a,b) than they do for the $(\bar{1}\bar{1}3)$ reflection (Figs. 7c,d). The only parameters which could have been changed are: (a) the magnitude of t, (b) the magnitude of s, and (c) both the magnitude and sign of the parameter $\bar{g}.\bar{R}$. A theoretical treatment of stacking fault images using absorption parameters suitable for the cases of the (200) and the (311) reflections in aluminum indicate that the defect visibility rules should hold for both beams at all values of s and for $\bar{g}\cdot\bar{R}$ either positive or negative.[19]

Without further theoretical and experiment treatment of this particular problem it is difficult to explain the behavior illustrated in Fig. 7, and which of the three parameters are responsible for this behavior. It has not been possible to obtain similar results in silicon. It would therefore probably be wise to attempt to apply this asymmetry property only to large defects, or, if to small defects, only when the extinction distance is small, i.e., only for low order reflections.

VI. DEFECT CHARACTERISTICS

Theories have already been developed for images from spherically-shaped defects and for platelike defects with strain vectors normal to

the defect plane.[1,2] Other systems may have defects which appear rod-shaped with radial strain fields or as prismatic loops whose Burgers vectors are far from normal to the loop plane. The Burgers vectors for most defects can usually be obtained without much trouble from $\bar{g}\cdot\bar{b}$ contrast experiments which also yield information on the shape and strain field of the defect.[8,10]

The dimensions of a defect are of considerable importance. A small defect can be so positioned in the foil as to be undetectable by strain contrast for a certain operative value of s whereas large defects will usually be spread out over a sufficiently large fraction or a large number of extinction distances to be detectable without difficulty. There is no upper size limit beyond which a defect cannot be imaged in strain contrast since imaging only depends on the ability of the defect to induce strain in the surrounding lattice in the direction of the operating reflection. The smaller the defect the more favorable must be the contrast conditions used for imaging; the use of large $\bar{g}\cdot\bar{b}$ values, an appropriate adjustment of the background intensity and the extinction distance, and fortune supplying defects close enough to the surface must be considered if the defects are very small.

In the case of platelike defects, consideration must be given to the effects upon the image which would be likely to occur due to orientation and inclination. In the cases of platelike precipitates or faulted loops with strain vectors normal to the plane of the defect the existing theory should be valid and the image profiles appropriate for defects inclined a few tens of degrees to the foil normal. However,

if the Burger's vector is inclined to the plane of the defect, as is common for a large number of perfect prismatic loops,[8,21] then severe complications can arise by attempting to apply the existing curves to the interpretation of defect images. One of these perfect prismatic loops with its Burgers vector in the plane of the foil would be, in cross-section, well approximated by an edge dislocation dipole. Cass[22] has developed a series of theoretical profiles for edge dislocation dipoles for wide variations in the parameters, w, separation, and depth in the foil. When the dipole of small separation is oriented such that its position in the foil and the macroscopic value of w provide a strong strain contrast image, then the black-white nature of the image is sensitive to the sense of slope of the plane of the dipole. Therefore, the character of a small prismatic loop oriented as prescribed cannot be determined from its strain contrast image because of the uncertainty in the sense of slope of the habit plane, there being generally more than one habit plane possible for a given Burgers vector. It is necessary in this case to orientate the specimen such that the Burgers vector and the normal to the habit plane are in the plane of the foil and to prove conclusively that this was the case, before statements concerning the nature of the defect can be made.

Defect density is another factor which can affect the results. Just as a stacking fault image can be affected by the presence of another fault above or below it or a dislocation image affected by the presence of another dislocation which forms a dipole, it is probable that the image of a small defect will also be affected either by the

proximity of other defects which modify the strain field of the first or by the existance of other defects above or below it, and the resulting micrograph may become a confused jumble of images or may contain images which are not truly representative of the nature of the defects. Defect images in quenched aluminum, quenched and aged Al-Mg_2Si, and Al-Cu contained in this paper illustrate this point well (see e.g. Figs 10, 12), for one would hesitate attempting to unambiguously identify the nature of the defects from some of these images. In a similar vein, the defect structure in heavily irradiated materials is also often confusing as to the nature of the defects present because of the tremendous amount of change in the imaging characteristics of the foils. In summary, when defects of only one kind produce mixed images, it is clear that trying to identify defects of mixed kinds is extremely difficult.

VII. DEFECT POSITION IN A FOIL

The position of the defect in the foil is perhaps one of the most important considerations. If it lies in the center of the foil, it will usually be undetectable by strain contrast unless the foil is relatively thin and s is quite near zero. If the defect lies on the surface it should be easily distinguishable by strain contrast and should appear in strong contrast in dark-field for only one sign of the parameter s. However defects on the surface are probably not representative of the defects introduced by a particular treatment for which it is desired to obtain information concerning the resulting defect

structure. Surface defects would more probably be introduced during preparation due to polishing conditions or handling. In the hexagonal Ag_2Al compound, deformed in tension, the defect structure is one in which there are broad slip bands containing high densities of perfect prismatic loops.[23] Between these bands there appear numerous small defects which were analysed as small polishing pits. These are shown in Fig. 8. Initially, the defect images showed, by comparing the bright-field and dark-field (obtained by gun tilting) micrographs, that they corresponded to images near the top surface, i.e. the white sides of the black white images were in both cases in the direction of the operating reflection. Upon turning the foil over and obtaining the same area and the same operating reflection, the dark-field images were the same and the bright-field images reversed, precisely as predicted by the theory for identical defects near the lower foil surface. This is precisely the behavior observed by Ruhle et. al.[16] for the case of defects introduced by unfavorable polishing conditions in undeformed, well-annealed copper foils. One further example is the rodlike defects in silicon illustrated in Fig. 9. These defects exhibit mass thickness contrast which indicate they are voidlike in nature. However, their strain contrast images specify that they have interstitial character. The dark-field images show that they can only be observed for one sign of s, that is, for $s < 0$ when they lie on the top surface of the crystal and for $s > 0$ when the foil is turned over. The bright-field images show the agreement in image characteristics expected on the basis of the two-beam theory. These defects are,

therefore, precipitates, or voids covered by an unknown residue of film, which has maintained the strain characteristics of the original defects.

A large defect lying inside the foil but intersecting the surface should be of an easily identifyable nature if no complications arise due to surface conditions such as preferential polishing of either the defect or the matrix, for example, an interstitial defect preferentially polished could exhibit vacancy image characteristics unless, as in the case of doped silicon above, (Fig. 9) a surface layer of polishing products or an oxide retained the strain in the lattice. In the case of plate shaped precipitates in an aluminum-4% copper alloy, all the θ' plates which are large enough to intersect the surface show vacancy type images, whereas the images from the smaller precipitates are quite ambiguous as to their character, as shown in Fig. 10.

We now turn our attention to those defects which occupy small localized regions in the interior of a foil, close enough to the surface to be suitable for detection by strain contrast imaging techniques, yet not on or intersecting the foil surfaces. These defects are the ones of greatest interest since they represent the microscopic defect structure of interest in materials. As has been shown theoretically, the image to be expected from a small defect depends critically upon its position or distance from the foil surface as measured in extinction distances of the operating reflection.[1,2] This image, if strong enough to be detected against the background intensity, can either be white or the side of the operating reflection for certain positions or black on the side of the operating reflection if the defect is half

an extinction distance above or below these positions.[1,2] This one fact, that a defect can exhibit either of two different images, is perhaps the greatest obstacle to conclusive identification of the nature of defects.

That such contrast reversals do occur can occasionally be shown with images of inclined dislocations and is illustrated using rodlike defects in silicon as shown in Fig. 11. Similar rodlike defects in Al-Mg_2Si, shown in Fig. 12, can exhibit a uniform type of contrast over large distances if they lie parallel to the foil surfaces or can be made to change contrast if they are slightly inclined and pass through a bend contour. If the defects are steeply inclined, they exhibit only very weak image reversals even at $s = 0$ in dark-field although they exhibit excellent dotted contrast at non-zero values of s. It should be mentioned that these defects are expected to be interstitial in character,[12] although a large number of the defects lying parallel to the surface exhibit vacancy type strain contrast images.

Strain contrast images of particular defects at given depths inside the foil can be made to change their black-white directions in a number of ways. Using the same reciprocal lattice vector as the operating reflection, s can be changed, thereby changing the effective depth of the defect in the foil, in terms of the extinction distance. This is illustrated for a number of defects in quenched aluminum in Fig. 13. Defects A and B reverse from $s = 0$ in dark-field going to $s < 0$; defect

C reverses from $s = 0$ going to $s > 0$, while defect D, not in good strain contrast at $s = 0$, reverses its image upon changing from $s < 0$ to $s > 0$. Further reversals of this type have been pointed out in Fig. 5. In Fig. 14 rodlike defects in silicon are shown which reverse their images upon changing the macroscopic value of s from zero to some positive value.

Alternatively, a different operating reflection can be used for contrast, which entails changing one or a number of the parameters important in imaging. The first is the parameter $\bar{g}.\bar{R}$ which may increase, decrease, remain the same or change sign with changing $\bar{g}$. Simultaneously, the extinction distance and the parameter s can change or remain the same. Quite often, changing $\bar{g}$ will entail changing all of these parameters. Figure 15 shows, for the case of rods in silicon, how images may appear by using first a high order reflection, the (400), and then a low order reflection, the (111). The two sets of images are obtained from the same region of the same foil but are not identical. Note that in each case the images can be made black on the side of the operating reflection for negative values of s and white for positive values of s, while at $s = 0$ the images for the two different reflections show entirely opposite character. Furthermore, comparison of Figs. 15e,f with Figs. 14a,b show that an entirely opposite behavior is encountered with the same defects under similar conditions, with the one exception that the foil has been turned over in the former case.(see also Fig. 17).

Changing to a reflection with a longer extinction distance is the recommended solution for causing defects, which are giving complications

in analysis of their character (i.e. having both black lobes and white lobes on the same side as $\bar{g}$), to exhibit an image from which the nature of the defect can be unambiguously determined. This indeed does appear to yield results, since Hesketh and Richards[24] have reported that the fraction of defects which yield "wrong" images decreases with increasing order of reflection. In Fig. 16, are shown some examples of defect images in quenched aluminum obtained using both low and high order reflections. The defects circled in (a) and (b) are those defects which reversed their black-white images upon changing the operating reflection from (200) to ($\bar{2}20$). Of the eight defects circled, one half of them have changed their apparent character from interstitial to vacancy and the other half do exactly the opposite, so no apparent advantage has been gained by using a higher order reflection for this foil. Furthermore, the ($\bar{2}20$) dark-field images are, in the great majority of cases, black on the side of the operating reflection. How to interpret the nature of these defects on the basis of strain contrast information is certainly unclear. Using the postulates of the strain contrast theory one would have to conclude that the defects in this quenched foil were primarily of interstitial character. This example is used to point out that, since the foil orientation is [001] and since most of the defects are perfect prismatic loops (as determined from the large number of double-arc images in the neighborhood),[21] that the orientation of the defect, the relationship between the Burgers vector and the defect plane, and the inclination of this plane to the operating reflection are parameters of considerable importance and must

be taken into account when analysing the defects. In the example (Fig. 16), the $\bar{g}\cdot\bar{b}$ product has changed from ±1 to ∓2 and the extinction distance has roughly doubled upon changing reflections. Even though the theoretical curves prepared by Cass[22] would be more appropriate than those based on single dislocation images, no conclusions regarding the precise nature of the defects can be reached because the slopes of their habit planes are uncertain. The sequence shown in Figs. 16c-g shows the defect A, in quenched aluminum with a much lower defect density, which analyses as interstitial in character for both the low order and the high order reflection, an analysis which is also invalid for the same reasons given above.

VIII. CORRESPONDENCE BETWEEN DARK-FIELD AND BRIGHT-FIELD IMAGES

The dynamical theory predicts that the black-white images of defects in the upper half of the crystal are similar in bright-field and dark-field while those of defects in the lower half of the foil are opposite in these two views.[1,2,6] This is a consequence of introducing absorption into the theory and there is an abundance of experimental evidence which illustrates this for defects at the surfaces, i.e. stacking fault fringes, slip-trace images, etch pit images etc. However, this relationship may not always hold for defects inside the foil. Consider the rodlike defects shown in Fig. 17; the dark-field, gun-tilted micrographs are shown with their corresponding bright-field aperture micrographs for the two cases of a foil before and after being turned over. Since the defects show opposite character in both sets,

they would always be analysed as lying in the lower half of the foil which cannot be unless we have the impossible situation of the defects being mobile inside the foil! A further complication entering here is the fact that the defect appears to have changed its character in that both the dark-field and the bright-field strain contrast images have changed in sense upon inverting the foil, in a manner expected for a screw dislocation in dark-field or for an edge dislocation in bright-field.[5,6]

Another interesting example which apparently contradicts the theory, in this respect, is illustrated in Fig. 18. Figures a and b are a bright-field, dark-field pair which contain a contour for either equal s or equal thickness (it is not clear which). A straightforward application of the theory by comparing strain contrast images yields the surprising result that all the defects above the contour are near the lower half of the foil while all defects showing strain contrast images in both views below the contour are near the top surface of the foil. Figures 18c,d are enlargements of the corresponding micrographs for area i and the triangles enclose easily comparable images. Since there are strain contrast images of some defects in bright-field appearing which do not have corresponding strain contrast images in dark-field, the argument may be entertained that the macroscopic value of s in this region is positive and hence only those defects near the bottom surface will appear. No such argument can be proposed to account for the images in region ii which is enlarged in Figs 18e,f. Every strain contrast image in bright-field has a corresponding strain contrast image

in dark-field. Hence the conclusion is forced that all defects showing strain contrast are near the upper surface, defects not showing strain contrast are near the center, and there are no defects near the lower surface. The circles enclose defects which lie near the upper surface and the squares enclose defects near the lower surface as determined from the dark-field, non-zero values of s, in the micrographs of the same region shown in Figs. 18g,h obtained using the $(\bar{2}20)$ reflection. Either the dark-field asymmetry rule[20] for defect contrast is completely invalid for the $(\bar{2}20)$ reflection or the predictions of the absorbing theory are wrong, in this instance, for strain contrast images. The thought that such a tremendous number of small defects distributed over such a large region of a quenched foil are all near one surface of the foil is quite unreasonable, so that there must be instances where the basic theory of electron diffraction breaks down. These cases are, admittedly, isolated and few, but the examples presented in this paper should be sufficient to prove that they occasionally occur.

IX. SUMMARY AND CONCLUSIONS

Some of the principal experimental conditions which affect the observation of strain contrast images have been investigated in detail. It is clear that correlation with existing theory is inadequate. The theory appears to work well for defects which approximate the theoretical models, i.e. those defects lying at or very near the foil surfaces, when observed at the Bragg angle with a suitable background intensity

present to permit strain contrast images to occur. It has been shown that often defects do not match the theoretical concepts, that is, there will be present a distribution of defects whose size, shape, strain field, degree of isolation, position and inclination could differ in varying degrees from the ideal.

Strain contrast imaging techniques do not seem to be generally applicable to the problem of distinguishing between vacancy and interstitial type defects, even when known defects are being investigated. However, it is possible, often by inspection, to determine the shape and direction of the displacement vectors of defects. Thus, loops, spherical clusters, plates, rods, and end-on dislocations can be distinguished from one another.[8] In addition, defects introduced "accidentally" at the surface of the foil can be recognized after suitable contrast experiments have been performed.

The principal factors affecting the utilization of strain contrast images are summarized in the following.

Oscillating images occur with depth, i.e. a given defect can give rise to two distinctly different images, thus, the precise position in the foil must be found before any conclusions as to the character of a defect can be reached.

The background intensity must be considered, and if not suitable, it must be adjusted. In general, the dark-field background intensity for thicknesses of odd-quarter extinction distances is one upon which strain contrast images can be easily detected; background minima in very thick foils can be used to yield weak strain contrast images only at the Bragg angle, whereas, background maxima can only be used

for non-zero values of the parameter s. The bright-field background behavior is similar only at or very near the Bragg angle, and it is generally not suitable for obtaining good strain contrast images when the incident electrons make an angle with the diffracting planes which is significantly larger or smaller than the Bragg angle.

In order to develop a theory which more closely corresponds to defects in a given system, it is necessary to use values of the extinction distance and the absorption distance appropriate for that system. Certainly, it would be most desirable to use experimentally determined values whenever possible, and to investigate the behavior of defects for a wide range of conditions by manipulating the various parameters involved. Perhaps in this manner, one could arrive at more reliable conclusions about the nature of defects present in a material.

Although it has been shown that the deviation parameter minimizes the applicability of the present theory by causing defects to reverse their apparent character, it is, nevertheless, felt that the electron microscopist can use this parameter to his advantage. With suitable theoretical preparation and sufficiently precise experimental control, it should eventually be possible to characterize the nature of defects as well as their position by studying their experimental behavior over a wide range of values of the parameter s.

Some slight advantage may be gained by going to higher order reflections in order to lengthen the extinction distance and thus lessen the probability of image reversal. However, it has been demonstrated that, not only can

image reversals occur with changing s, but also the range of useful diffracting conditions is markedly hampered for these cases. Higher order reflections often result in poor image quality, not to mention the fact that the scattering power, and hence the scattering intensity, is often quite low. This latter point is not taken into account in the present theory.

Finally, it has been demonstrated that occasionally the two-beam diffracting theory in absorbing crystals may not be entirely correct in predicting defect images and, thus, it is not surprising that it is sometimes difficult or impossible to completely identify defect characteristics.

ACKNOWLEDGEMENTS

We appreciate the continued financial support of our work by the U.S. Atomic Energy Commission. Thanks are due to P. R. Okomoto, E. Levine and J. L. Strudel for making some foils available for this investigation.

FIGURE CAPTIONS

Figure 1 (a) Normal bright-field and (b) aperture dark-field images of a wedge-shaped quenched aluminum foil (g=(111), foil normal [1$\bar{1}$0]) dependence of the background intensity on foil thickness. Inserts demonstrate poor strain contrast imaging at integral numbers of extinction distances except in thicker foils in dark-field. Optimum background occurs in all cases at odd-quarter number of extinction distances.

Figure 2 Theoretical wedge foil intensity profiles at the Bragg condition based on measured absorption parameters in aluminum for the reflecting planes: (a) (111), (b) (200), (c) (220), (d) (311). Abscissae are multiples of (111) extinction distances.

Figure 3 Effect of the deviation parameter on theoretical wedge foil intensity profiles for (111) in aluminum. (a), (b), (c) are bright-field profiles for w = -0.5, w = 0, w = +0.5, respectively. (d) and (e) are dark-field profiles for w = 0 and w = ±0.5, respectively.

Figure 4 Dark-field micrographs of a bent, wedge-shaped quenched aluminum [1$\bar{1}$0] foil for (a) (111) reflection and (b) (220) reflection, illustrating the greater restriction upon the deviation parameter s with higher order reflections for obtaining defect images.

Figure 5 Defect images in a quenched aluminum [001] foil for the various experimental conditions: (a) bright-field s = 0 for the (200) reflection, (b) gun-tilt dark-field, s = 0, for the ($\bar{2}$00) reflection, (c) same, s <0, (d) same, s >0, (e) gun-tilt dark-field, s = 0, for the (220) reflection.

Figure 6 Dark-field gun-tilt defect images in a quenched aluminum [1$\bar{1}$0] foil for the various values of s shown for (a) the (111) reflection (b) the (220) reflection. Arrows indicate directions of the operating reflections; mark is 0.1 micron.

Figure 7 Gun-tilt dark-field defect images for a quenched [031] aluminum foil. (a) and (b) are s < 0 and s > 0 micrographs for the (200) reflection; (c) and (d) those for the (113) reflection, illustrating ambiguity in determining some defect positions using non-zero values of s for imaging conditions.

Figure 8 (a) Normal bright-field and (b) gun-tilt dark-field images of defects in Ag_2Al; (c) and (d) the same, respectively, after inverting the foil. Images indicate that the defects are only on or near one surface of the foil and are probably a result of unfavorable polishing conditions.

Figure 9 Same imaging conditions as Fig. 8. Rodlike defects in doped silicon lie on the surface and exhibit voidlike absorption contrast and interstitial strain contrast.

Figure 10 θ^1 plates and G.P. zones in aluminum-copper; dark-field, gun-tilt image. The largest plates show uniformly vacancy-type strain contrast and probably intersect the foil surfaces. The smaller defects show both interstitial and vacancy type strain contrast images.

Figure 11 Illustrating contrast reversals along an inclined rod-like defect in doped silicon. Gun-tilted dark-field image.

Figure 12 Rodlike defects in Al-Mg_2Si observed in gun-tilted dark-field using the (111) reflection. (a) Defects can extend over avery large distance without exhibiting any contrast reversal if they are relatively parallel with the foil surface or (b) slightly inclined defects can be caused to exhibit reversal in the region of a bend contour. (c) An inclined rod in this system shows only weak contrast reversals even at the Bragg condition and (d) exhibits strong dotted contrast at $s > 0$.

Figure 13 Defect images in a quenched aluminum [001] foil for the various experimental conditions: (a) bright-field, $s = 0$, for the (200) reflection, (b) gun-tilt dark-field, $s = 0$, for the $(\bar{2}00)$ reflection, (c) same, $s <$), (d) same, $s > 0$, illustrating contrast reversals which occur by changing the sign of the parameter s.

Figure 14 Images of defects in doped silicon which reverse their black-white images with changing s in dark-field, (a) $s = 0$, (b) $s > 0$.

Figure 15 Defect image reversals in doped silicon with changing g and s in dark-field. (a), (b), and (c) are for $s < 0$, $s = 0$ and $s > 0$, respectively, for the (400) reflection while (d), (e), and (f) are the same for the (111) reflection.

Figure 16 Defect images in quenched [001] aluminum foils. (a) and (b) are gun-tilted dark-field images for the reflections shown; the circled images are those which reverse their black-to-white directions with respect to the operating reflection. The series (c) bright-field, $s = 0$, (d) dark-field, $s = 0$, (e) same, $s < 0$, (f) same, $s > 0$, and (g) gun-tilt dark-field, $s = 0$, for the (220) reflection, demonstrate a sequence for analyzing the defect A as being of interstitial character using the present theory.

Figure 17 (a) Gun-tilt dark-field images and (b) Aperture bright-field images of defects in doped silicon; (c) and (d) the same, respectively, after inverting the foil. From their images, the defects would always be analysed as being in the lower half of the foil.

Figure 18 (a) Normal bright-field and (b) gun-tilt dark-field images of defects in a quenched aluminum; [001] foil. Comparison of the images above the contour indicates that all defects in this region are at the bottom of the foil, while all the defects below the contour are at the top of the foil. (c) and (d) are corresponding enlargements from

(Figure 18 continued)

area i, the triangles enclose comparable images. (e) and (f) are enlargements from area ii; the circles enclose defects which are near the upper surface and the squares those near the lower surface as determined from the dark-field gun-tilt micrographs for the ($\bar{2}20$) reflection: (g) $s < 0$, (h) $s > 0$.

REFERENCES

1. M. F. Ashby and L. M. Brown, Phil. Mag., 8 1063 (1963).

2. M. F. Ashby and L. M. Brown, Phil. Mag., 8 1649 (1963).

3. See e.g. A. Kelly and R. B. Nicholson, Prog. Mat. Sci., 10 149 (1963).

4. P. B. Hirsch, A. Howie and M. J. Whelan, Phil. Trans. Roy. Soc. A252 499 (1962).

5. A. Howie and M. J. Whelan, Proc. Roy. Soc. A263 217 (1961).

6. A. Howie and M. J. Whelan, Proc. Roy. Soc. A267 206 (1962).

7. G. Thomas, Thin Films (ASM) p. 227 (1964).

8. G. Thomas and W. L. Bell, "Identification of Prismatic Dislocation Defects by Electron Microscopy", Proc. of Honolulu Conf. on Lattice Defects 1965; Gordon and Breach in press.

9. W. J. Tunstall, P. B. Hirsch and J. Steeds, Phil. Mag. 9, 99 (1964).

10. W. L. Bell, D. M. Maher and G. Thomas, Lattice Defects in Quenched Metals, Academic Press N.Y. 1965 p. 739.

11. U. Essmann and M. Wilkens Phys. Stat. Solidi 4 K53, (1964).

12. G. Thomas, J. Inst. Metals 90, 57 (1961-62).

13. G. Thomas and W. L. Bell, International Electron Microscopy Conference, Kyoto, Japan (1966).

14. D. W. Pashley and A. E. B. Presland, Phil. Mag. 6 1003 (1961).

15. L. M. Howe, R. W. Gilbert and G. R. Piercy, Appl. Phys. (Letters) 3 125 (1963).

16. M. Ruhle, M. Wilkens and U. Essmann, Phys. Stat. Solidi 11 819 (1965).

17. H. Hashimoto, A. Howie and M. J. Whelan, Proc. Roy. Soc. A269 80 (1962).

18. H. Hashimoto, A. Howie and M. J. Whelan, Phil. Mag. 5 967 (1962).

19. W. L. Bell unpublished results.

20. W. L. Bell and G. Thomas, Phys. Stat. Solidi 12 843 (1965).

21. W. L. Bell and G. Thomas, Phil. Mag. 13 395 (1966).

22. T. R. Cass, Ph. D. Thesis, Univ. of California, Berkeley (UCRL 11996).

23. P. R. Okamoto, M.S. Thesis, Univ. of California, Berkeley (UCRL 16957).

24. R. V. Hesketh and G. K. Richards, Phil. Mag. 13 1069 (1966).

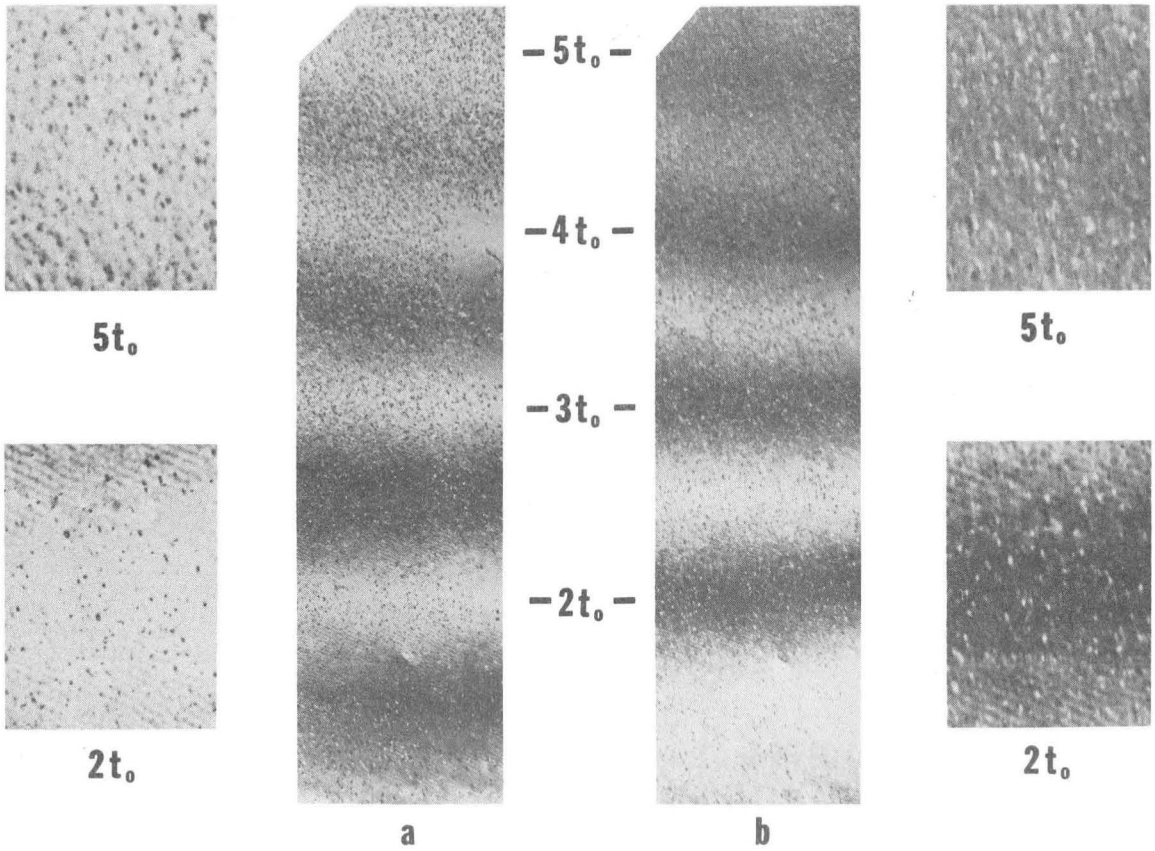

ZN-5709

Fig. 1

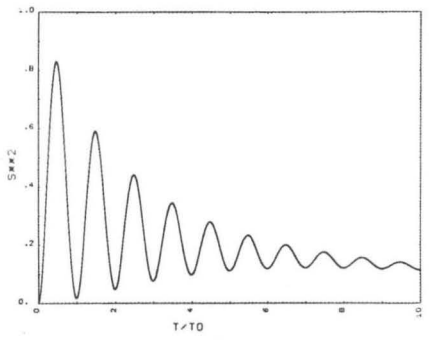

a

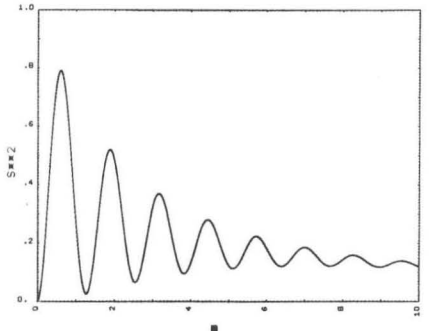

b

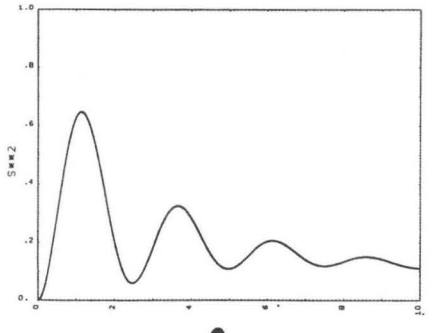

c

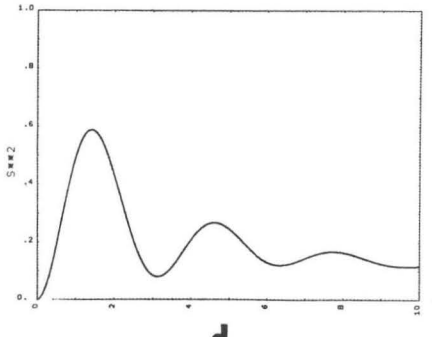

d

MUB 12623

Fig. 2

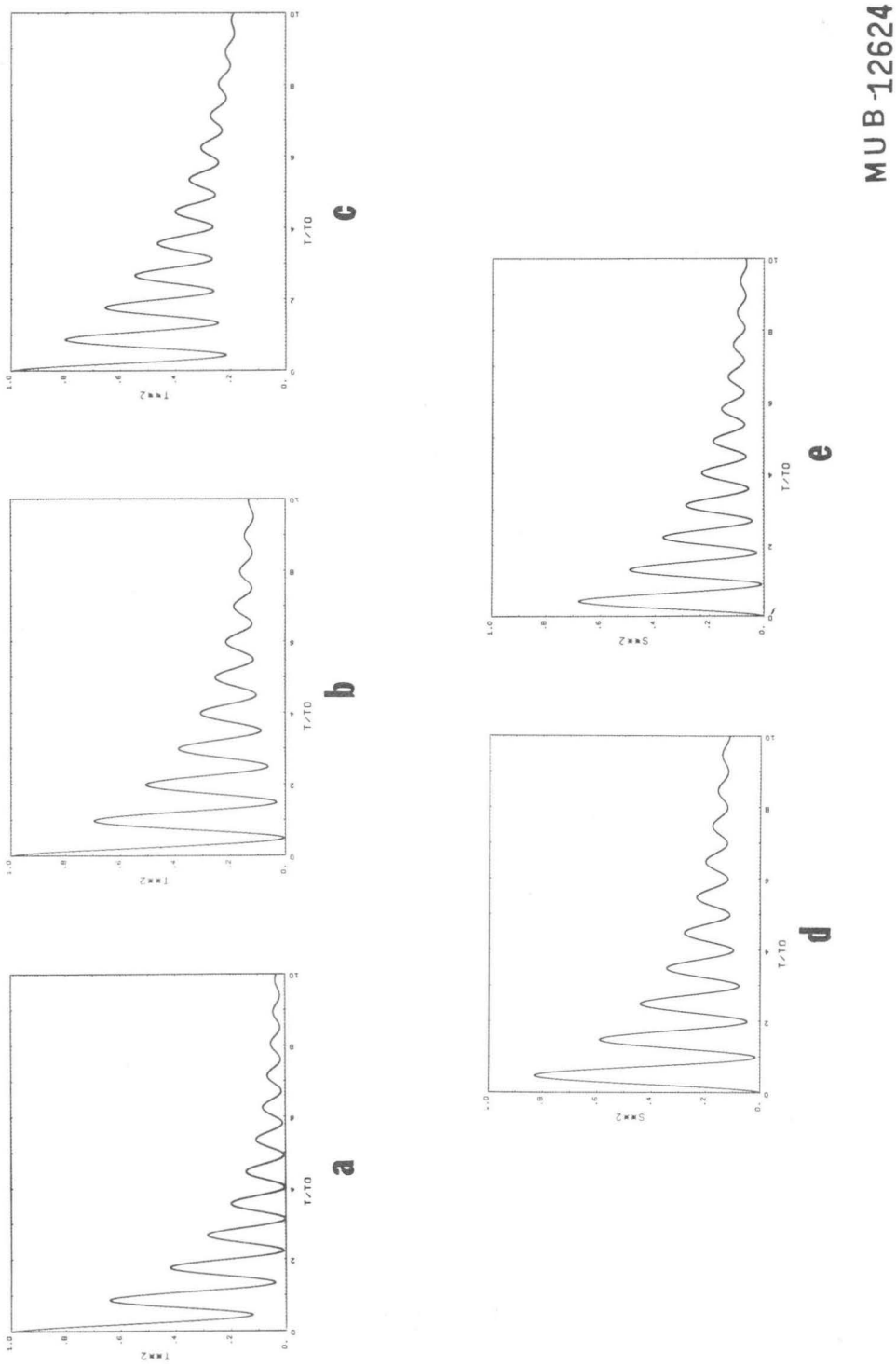

Fig. 3

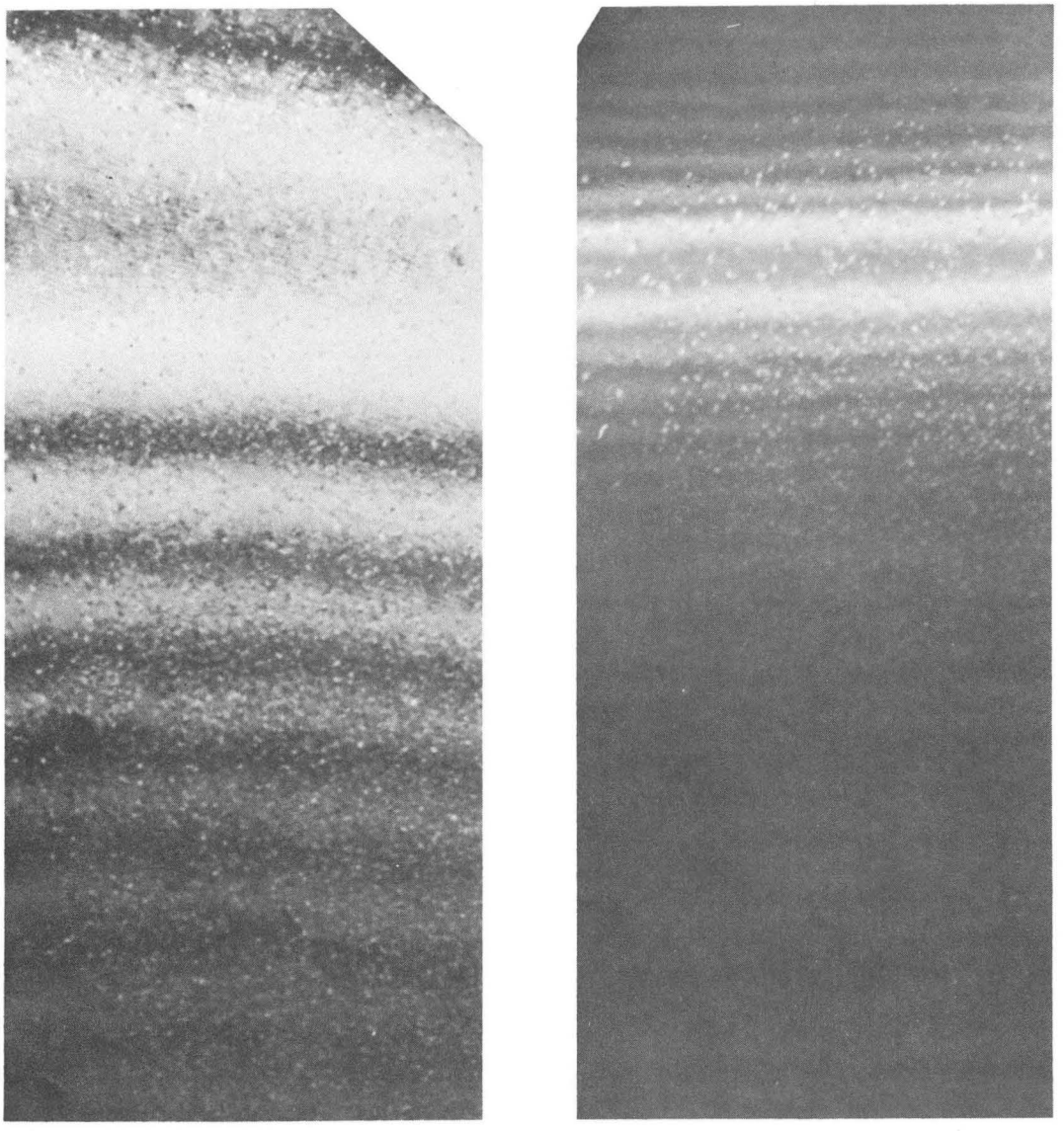

a b

ZN-5712

Fig. 4

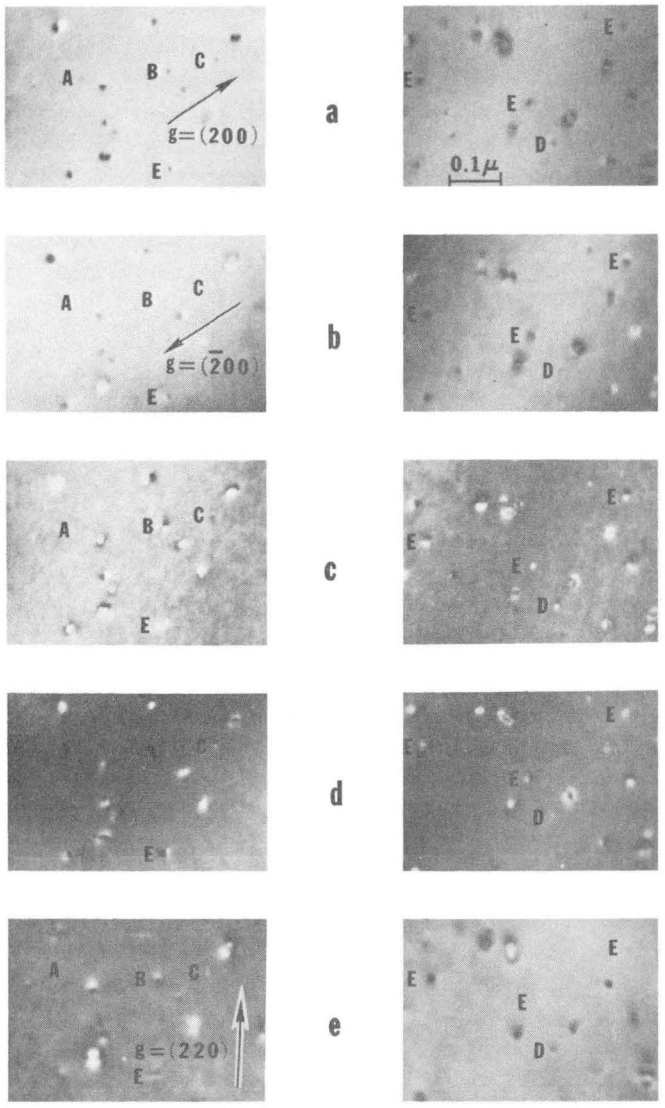
A
B
C
g=(200)
E
a
E
E
E
D
0.1μ
A
B
C
g=(2̄00)
E
b
E
E
E
D
A
B
C
E
c
E
E
E
D
E
d
E
E
D
A
B
C
g=(220)
E
e
E
E
E
D

ZN-5713

Fig. 5

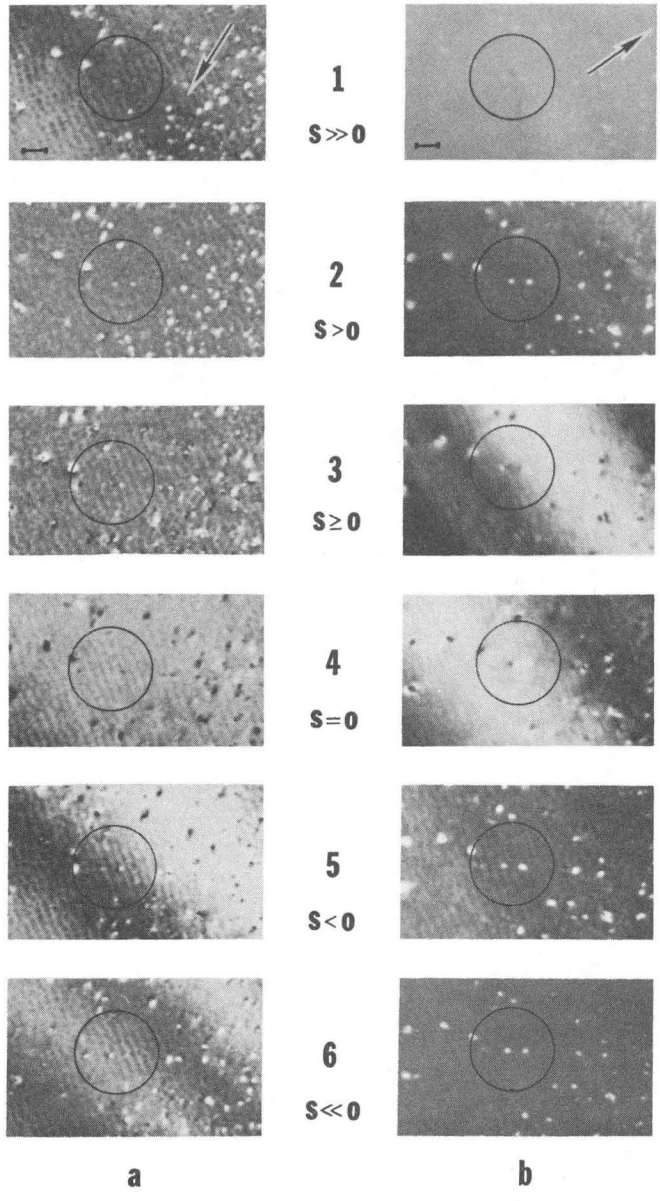

ZN-5714

Fig. 6.

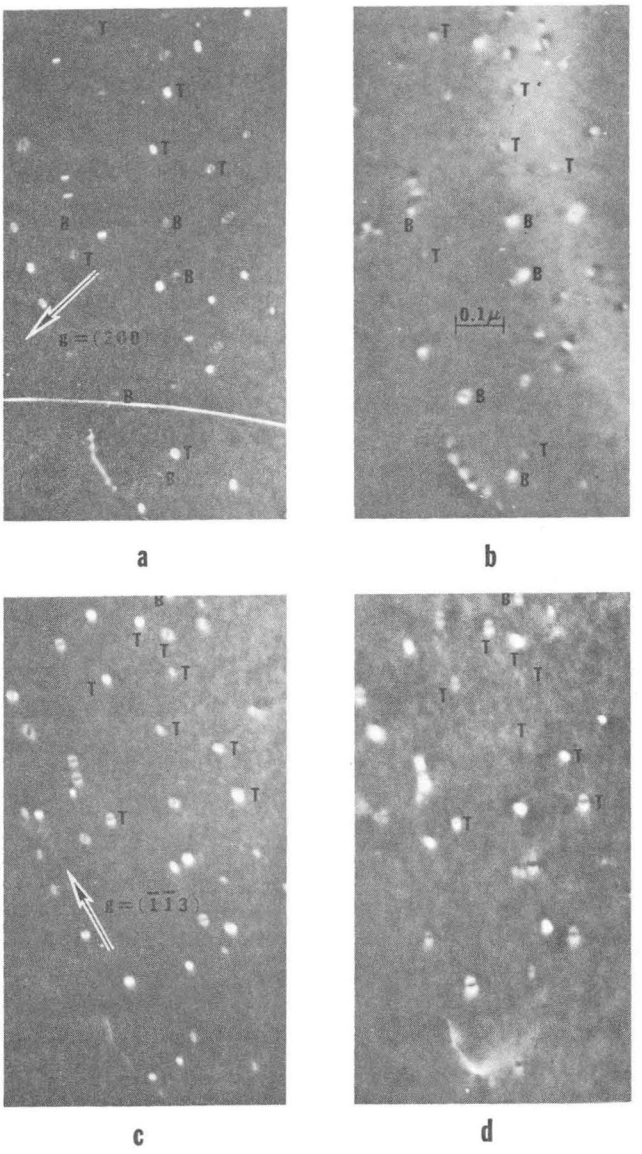

ZN-5715

Fig. 7.

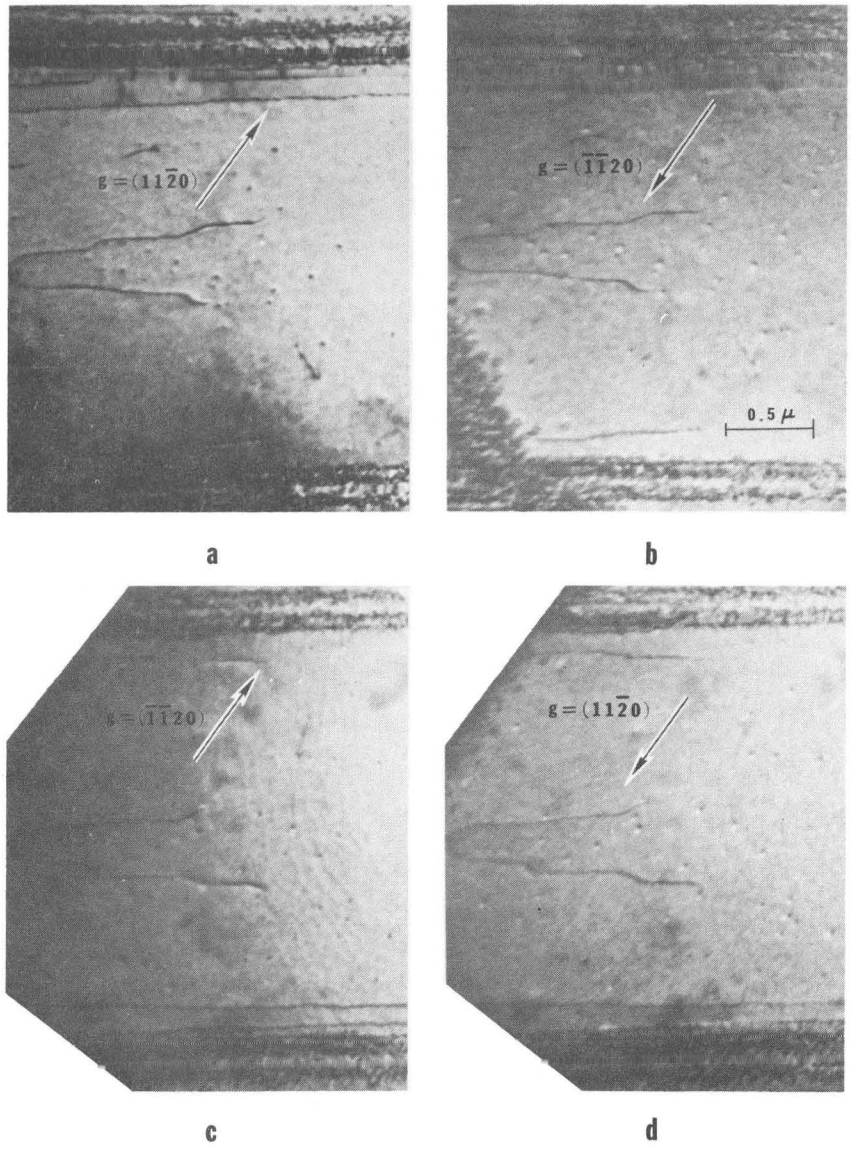

ZN-5716

Fig. 8.

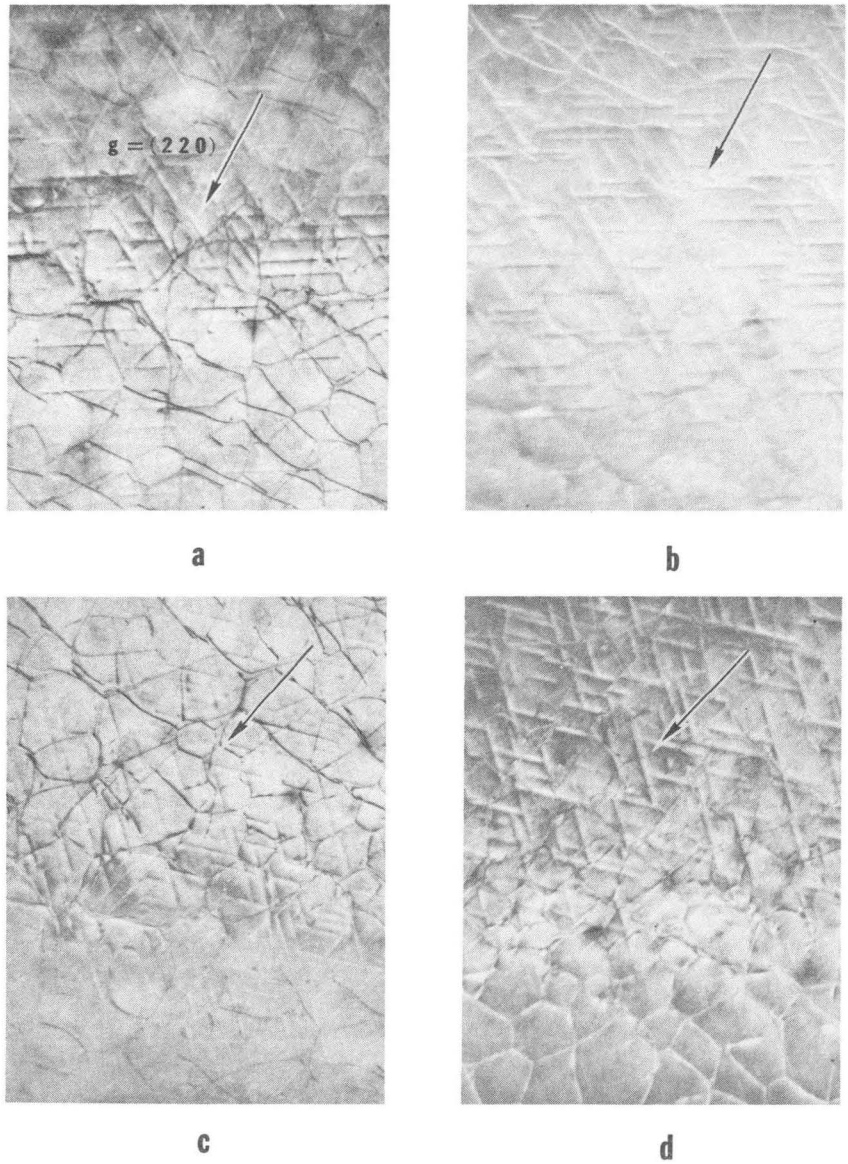

ZN-5717

Fig. 9.

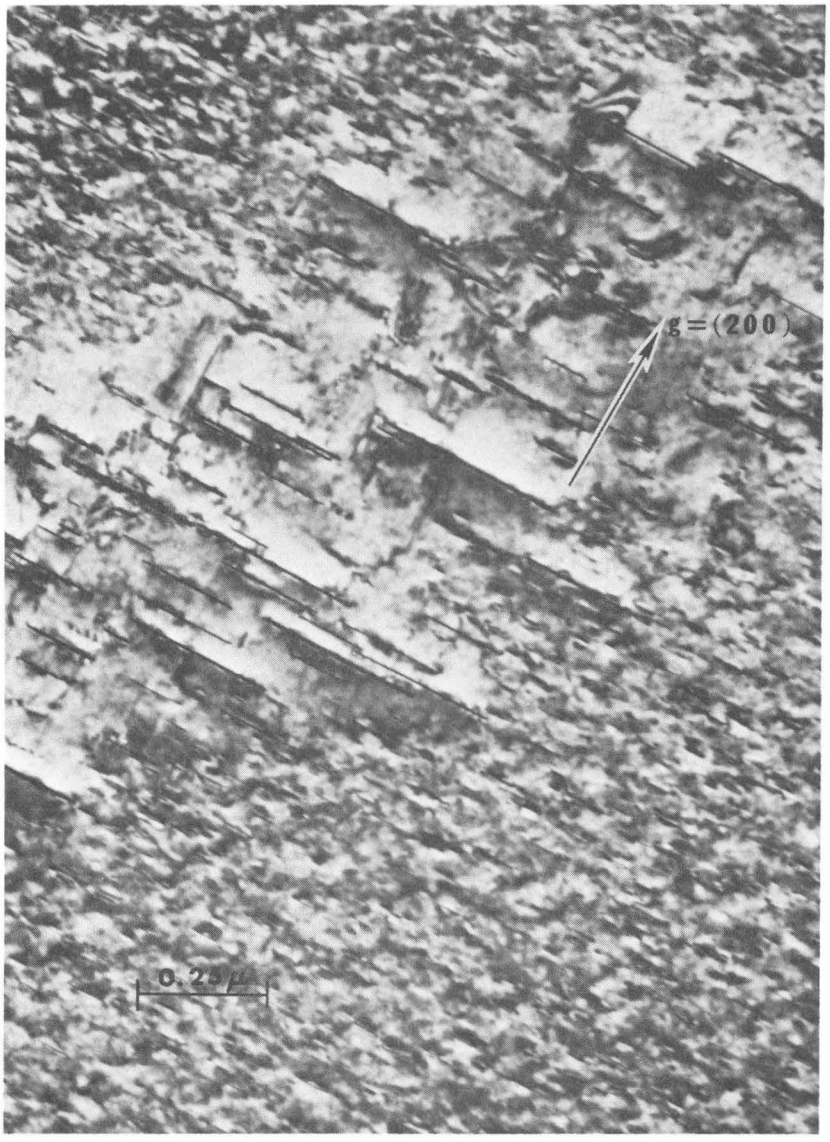

ZN-5718

Fig. 10

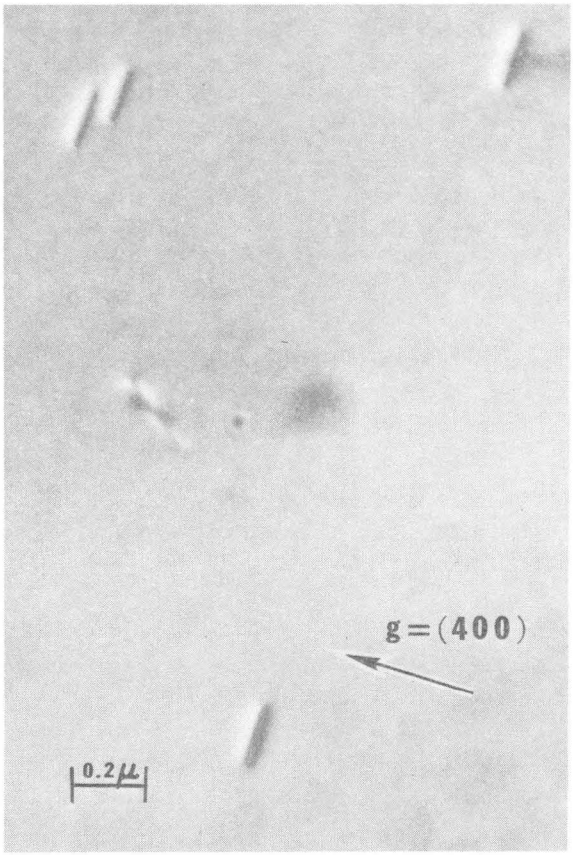

ZN-5719

Fig. 11

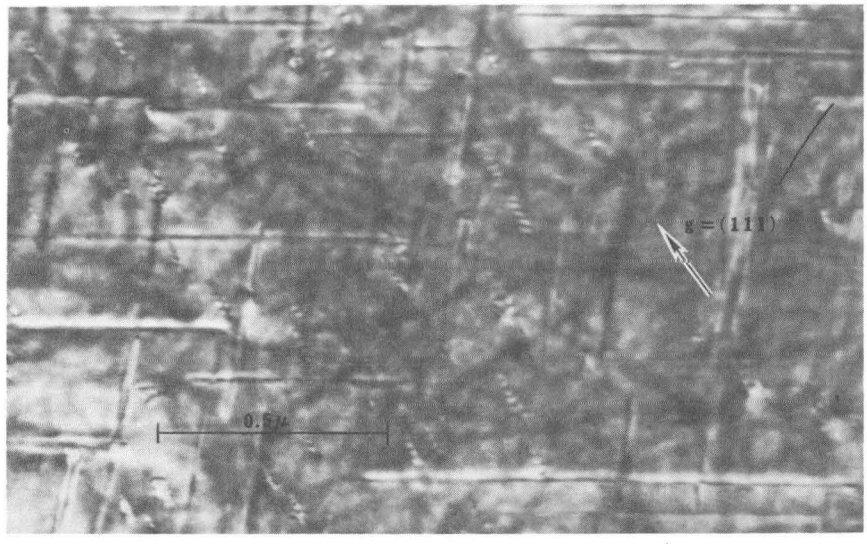

a

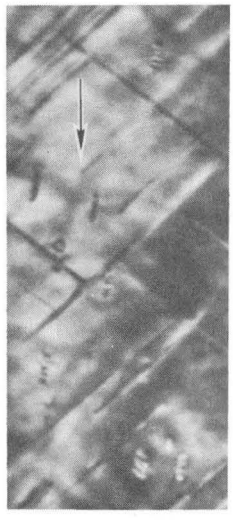

b

c

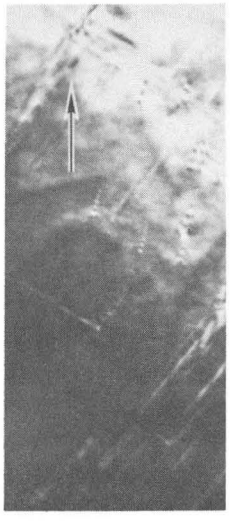

d

ZN-5720

Fig. 12

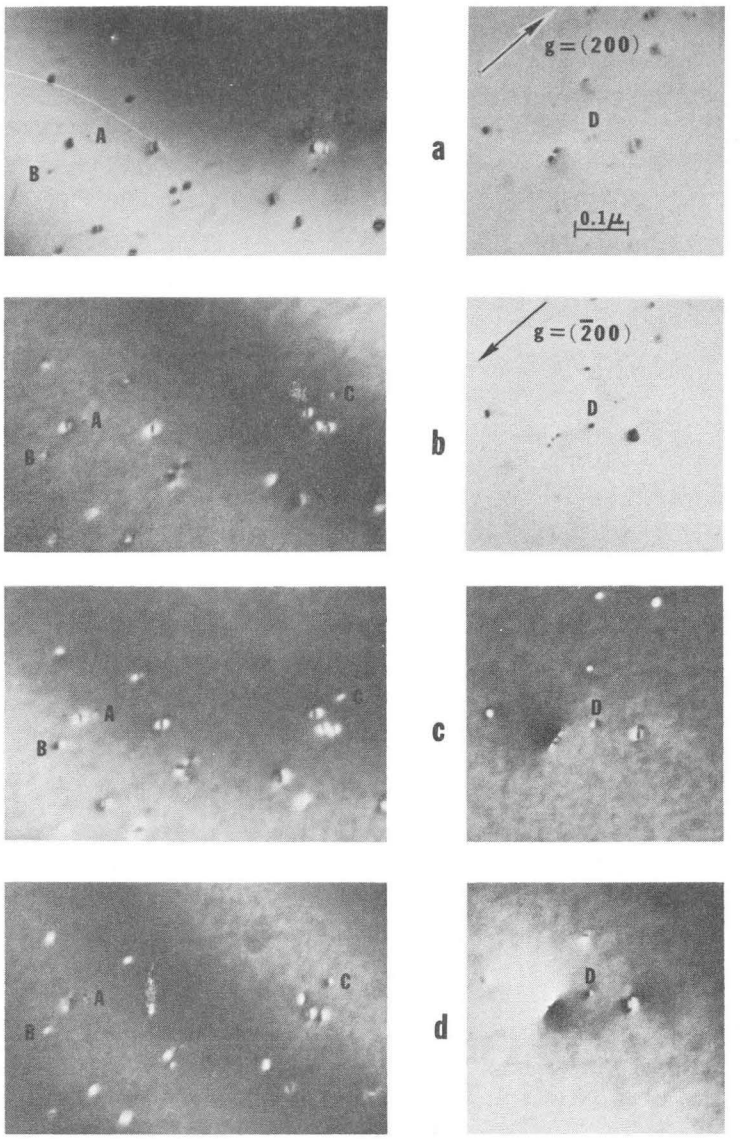

ZN-5721

Fig. 13

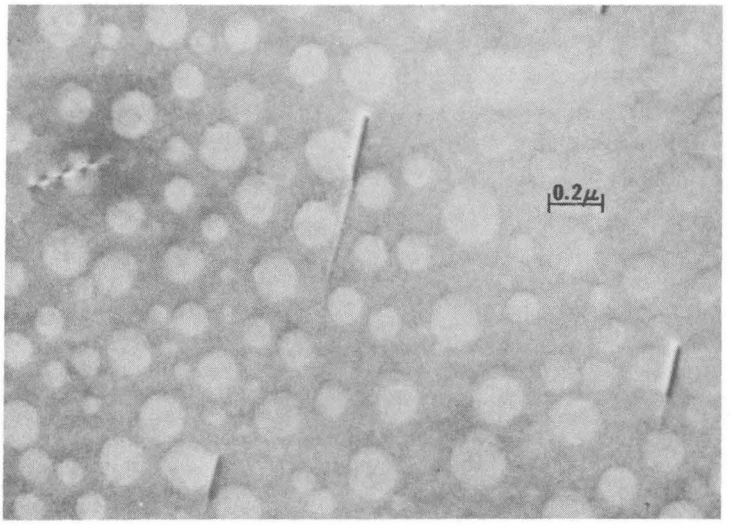

a

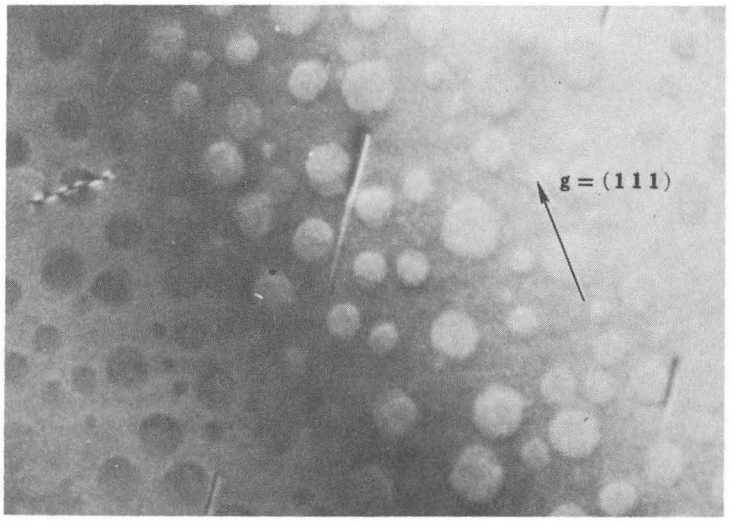

b

ZN-5722

Fig. 14

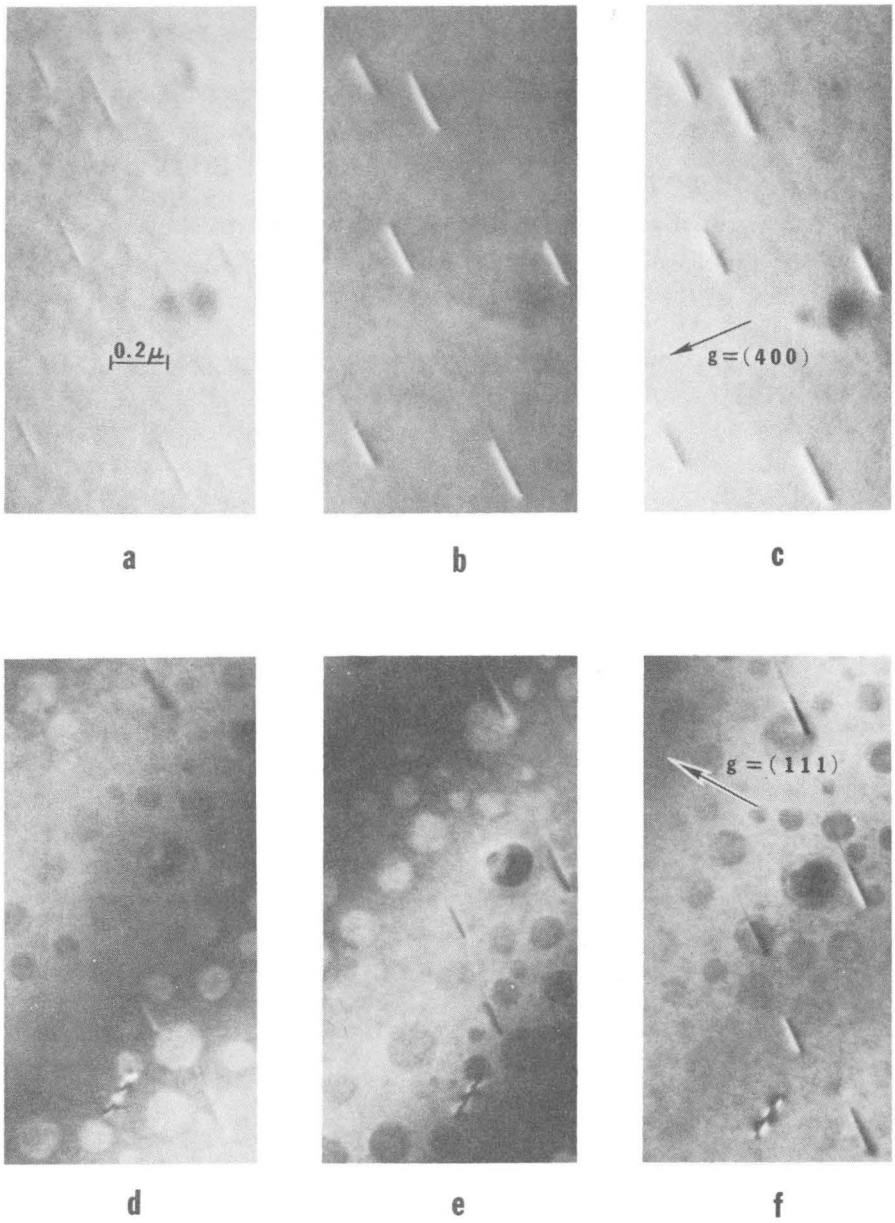

ZN-5723

Fig. 15

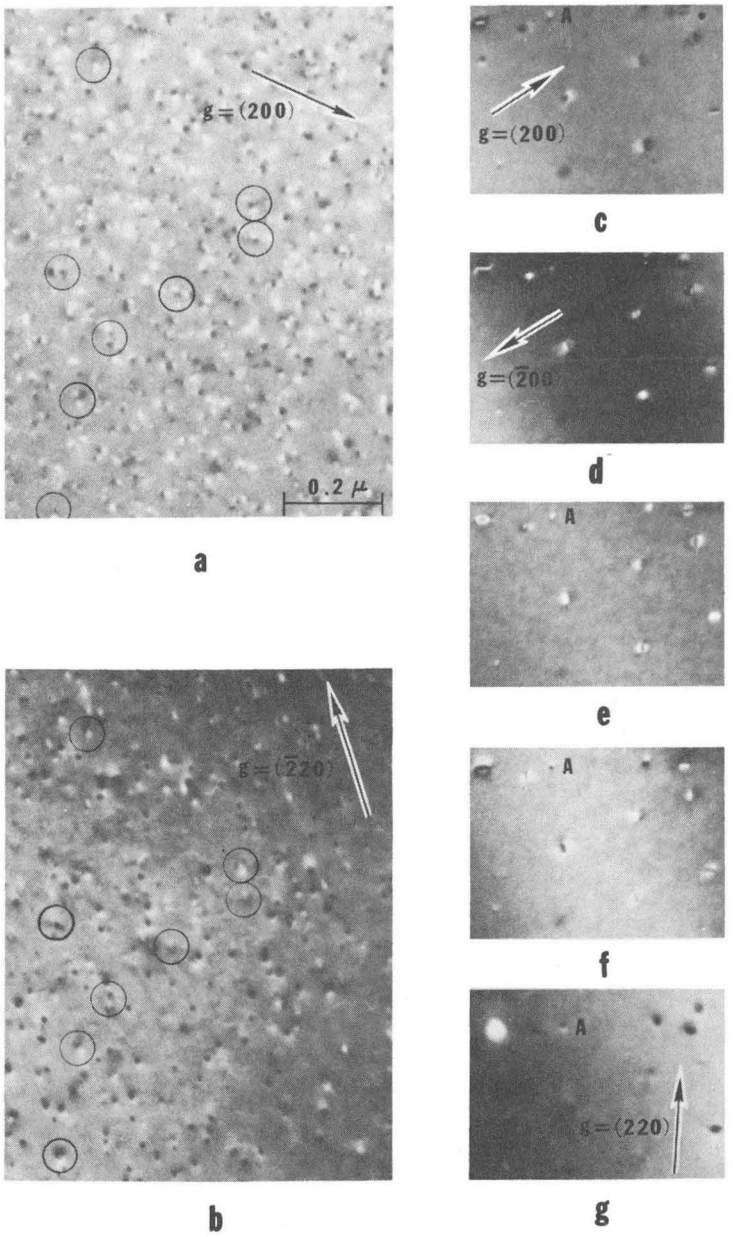

ZN-5724

Fig. 16

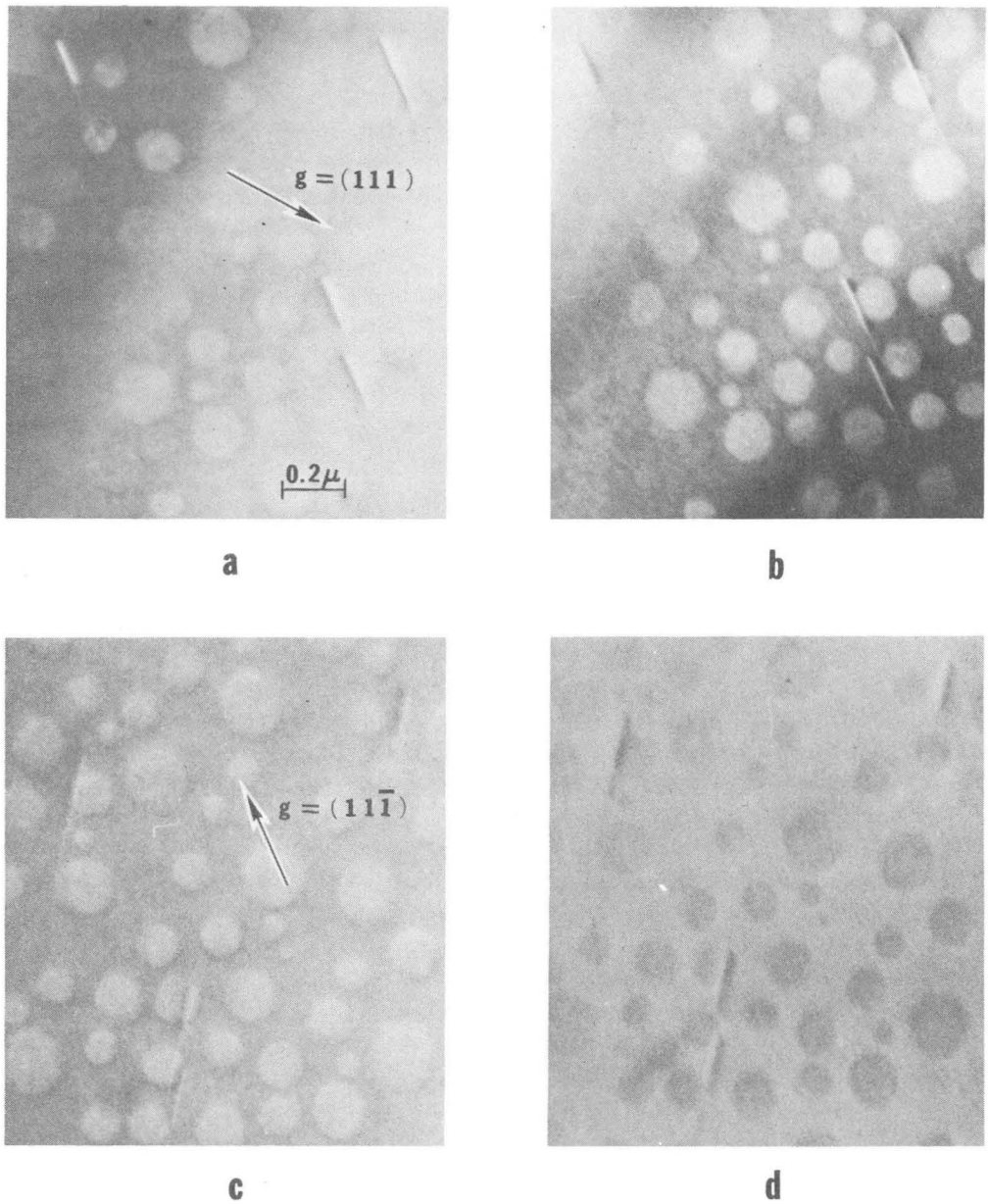

ZN-5725

Fig. 17

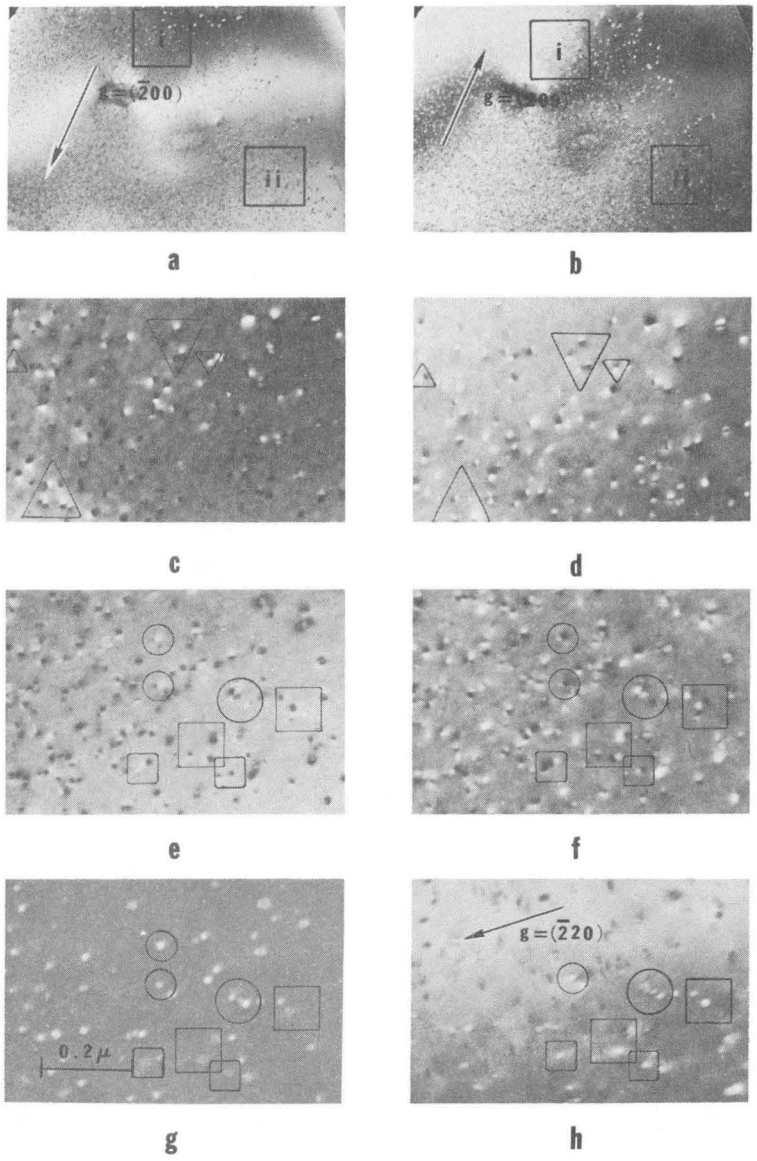

ZN-5726

Fig. 18

This report was prepared as an account of Government sponsored work. Neither the United States, nor the Commission, nor any person acting on behalf of the Commission:

A. Makes any warranty or representation, expressed or implied, with respect to the accuracy, completeness, or usefulness of the information contained in this report, or that the use of any information, apparatus, method, or process disclosed in this report may not infringe privately owned rights; or

B. Assumes any liabilities with respect to the use of, or for damages resulting from the use of any information, apparatus, method, or process disclosed in this report.

As used in the above, "person acting on behalf of the Commission" includes any employee or contractor of the Commission, or employee of such contractor, to the extent that such employee or contractor of the Commission, or employee of such contractor prepares, disseminates, or provides access to, any information pursuant to his employment or contract with the Commission, or his employment with such contractor.